through rainwater impounding alone will be effective to reclaim the tsunami-affected agricultural lands[15]. Hence, agricultural lands under situation I can be easily reclaimed considering the higher annual rainfall (>3000 mm), which can be effectively used for leaching out the accumulated salts. However, the areas under situation II require construction of raised embankments along with sluice gates, which will regulate the ingress of sea water in these areas. It will restrict the entry of sea water into the field during high tide and will allow the drainage of rainwater from the field, which may collect during the rainy season during low tide. In case of situation III (Permanent stagnation of sea water and depth of impounding increases with high tide), it has been envisaged that brackish-water aquaculture would be an alternative livelihood option.

Besides these, a set of agronomic management practices as enlisted below may be followed for effective rehabilitation of salt-affected soils.

- Selection and raising of salt-tolerant varieties of crops like rice, sugarcane, sorghum, watermelon and forage crops like karnal grass (*Diplachne fusca*) and para grass (*Brachiaria mutica*), and green manure crop like *Sesbania* sp.
- Selection of suitable crop rotation like rice–watermelon, rice–maize, rice–sorghum, rice–vegetables, rice–sugar beet and rice–forage crops.
- Adoption of broad bed and furrow system of land manipulation in the affected areas
- Application of higher dose of farmyard manure (FYM) to improve the physical condition of the soil and drainage.
- In case of rice, transplanting of aged seedlings of salt-tolerant variety and increased number of seedlings (4–6) per hill.
- Sowing seeds in the furrows or two-thirds from the top of the ridge.
- For wide-spaced crops like vegetables, adoption of the pit system of planting by replacing the salt-affected soil with a mixture of normal soil and FYM.
- Adoption of frequent light irrigation.
- Adoption of drip irrigation or pitcher irrigation for high-value crops.
- Application of higher dose of NPK than the recommended dose, and
- Adoption of auger hole technique for planting tree species in salt-affected areas.

1. Navalgund, R. R., Sumatra tsunami of December 26, 2004. *J. Indian Soc. Remote Sensing*, 2005, **33**, 1–6.
2. Velmurugan, A., Swarnam, T. P. and Ravisankar, N., Assessment of tsunami impact in South Andaman using remote sensing and GIS. *J. Indian Soc. Remote Sensing*, 2006, **34**, 193–202.
3. Somani, L. L., *Crop Production with Saline Water*, Agro Botanical Publishers, Bikaner, 1991, p. 308.
4. Datta, K. K. and De Jong, C., Adverse effect of water logging and soil salinity on crop and land productivity in northwest region of Haryana, India. *Agric. Water Manage.*, 2002, **57**, 223–238.
5. Page, A. L., Miller, R. H. and Keeney, D. R. (eds), In *Methods of Soil Analysis, Part II, Chemical and Microbiological Properties*, ASA, SSSA, Madison, Wisconsin, USA, 1982.
6. USSL STAFF, Diagnosis and improvement of saline and alkali soils. *USDA Hand Book No. 60*, 1954, p. 147.
7. Ganeshamurthy, A. N., Dinesh, R., Ravisankar, N., Anil Nair and Ahlawat, S. P. S., *Land Resources of Andaman and Nicobar Islands*, Central Agricultural Research Institute, Port Blair, 2002, p. 134.
8. Rachman, A., Wahyunto and Agus, F., Integrated management for sustainable use of tsunami affected land in Indonesia. Paper presented at the Mid-term Workshop on Sustainable use of Problem Soils in Rainfed Agriculture, Khon Khaen, Thailand, 14–18 April 2005.
9. Gupta, I. C. and Abhichandani, C. T., Seasonal variations in salt compositions of some saline water irrigated soils of Western Rajasthan. *J. Indian Soc. Soil Sci.*, 1970, **18**, 428–435.
10. Pal, B. and Tripathi, R. K., Physico-chemical characteristics of soils of a semi-desert tract of UP as affected by irrigation water quality. *J. Indian Soc. Soil Sci.*, 1979, **27**, 240–248.
11. Manchanda, H. R. and Chawla, K. L., Soil profile variations and wheat growth under irrigation with highly saline waters in coarse loamy soils in South Western Haryana. *J. Indian Soc. Soil Sci.*, 1981, **29**, 504–511.
12. AICRP, ICAR All India Coordinated Research Project on Management of Salt-affected Soils and Use of Saline Water in Agriculture, 1972–1993. Annual Reports, CSSRI, Karnal, 1994.
13. Minhas, Saline water management for irrigation in India. *Agric. Water Manage.*, 1996, **30**, 1–24.
14. Zeng, L., Shannon, M. C. and Lesch, S. M., Timing of salinity stresses affects rice growth and yield components. *Agric. Water Manage.*, 2001, **48**, 191–206.
15. Gupta, S. K., Ambast, S. K., Gurbachan Singh, Yaduvanshi, N. P. S., Ghoshal Chaudhuri, S. and Raja, R., Technological options for improved agriculture in tsunami affected Andaman & Nicobar Islands and Maldives. Central Soil Salinity Research Institute, Karnal, 2006, p. 88.

Received 22 April 2008; revised accepted 23 October 2008

Intensity of shape preferred orientation in a granite and its tectonic implications

Sukhen Majumder and Manish A. Mamtani*
Department of Geology and Geophysics,
Indian Institute of Technology, Kharagpur 721 302, India

The present study deals with the measurement of intensity of shape preferred orientation in the Palaeoproterozoic Malanjkhand Granite (Central India). This intensity is measured by calculating the strength of mineral lineation of biotite (K_{bi}). The NE–SW striking Central Indian Suture (CIS) that was formed by the collision of the Bundelkhand and Bastar cratons lies to the north of the granite and K_{bi} was calculated in 11 samples collected at varying distances from the

*For correspondence. (e-mail: mamtani@gg.iitkgp.ernet.in)

CIS. The data indicate that κ_{bi} increases towards the CIS. Therefore, it is concluded that tectonic events associated with the CIS have influenced fabric development in the Malanjkhand Granite. Previous studies about the timing of formation of the CIS are described and the time-relationship between fabric development in the Malanjkhand Granite and regional tectonics is discussed.

Keywords: Fabric, granite, shape preferred orientation, tectonics.

STUDIES on granites during the past few decades have revealed that many granitic plutons emplace and develop fabrics synchronously with regional deformation[1,2]. Also, emplacement of several granite plutons is known to be associated with transpressional tectonics, evolution of shear zones or tectonic rejuvenation of existing shear zones[3–5]. In India, the Godhra Granite in the Aravalli Mountain Belt is known to have emplaced syntectonically with the Grenvillian-age tectonic rejuvenation of the Central Indian Tectonic Zone (CITZ) that lies to the south of the granite[6]. Analysis of deformation fabric using anisotropy of magnetic susceptibility (AMS) as well as intensity of shape preferred orientation (SPO) in the Godhra Granite has revealed that strain in the granite is higher in samples proximal to the CITZ[7,8]. Thus, it is known that the intensity of SPO can vary in granitic plutons, which can be linked to regional strain intensity variations.

In the present study, the intensity of SPO was measured in the Malanjkhand Granite (Central India), which is ~2.48 Ga in age[9]. It is a grey granite in which quartz, plagioclase, K-feldspar, biotite and sometimes hornblende are the main minerals, while sphene, pyrite, magnetite, ilmenite and zircon occur as accessory minerals. The granite has proximity to the Central Indian Suture (CIS) that lies to its north (Figure 1). The CIS forms the southern boundary of the CITZ that is known to have formed by the accretion of the Bundelkhand and Bastar cratons[10]. According to few workers, the CITZ evolved between 2.4 and 1.8 Ga, and experienced at least three tectonothermal events at ~1.8, ~1.5 and ~1.0 Ga. Each event was characterized by collisional tectonism and crustal recycling[11] and the final suturing of the Bundelkhand and Bastar cratons occurred at ~1.5 Ga. However, palaeomagnetic studies[12,13] indicate that the CIS formed between 2.5 and 1.8 Ga. Since the Malanjkhand Granite lies to the south of the CIS and its age is ~2.48 Ga, it is likely that the fabric in the granite has been influenced by the tectonic evolution of the CIS[9].

In the vicinity of the CIS, mylonites are recorded in the granite. Similar mylonites are absent in the central and southern parts of the granite. Central parts of the granite show preferentially oriented feldspar laths, which indicates fabric development in the magmatic state[14,15]. Microstructural studies of rocks from the central part of the granite reveal the presence of high-T solid-state deformation fabrics, such as chess-board pattern in quartz[16,17]. In contrast, the northern part of the granite shows low-T fabrics, such as bulging grain boundaries in quartz[18]. Thus, there is a superimposition of low-T over high-T fabrics in the granite, which is prominent in the northern part; the latter has proximity to the CIS. The above field and microstructural evidences indicate that there could be a relationship between fabric development in the Malanjkhand Granite and tectonic events associated with CIS formation. However, this time-relationship was not investigated in the past. In the present study, the intensity of SPO was measured in several Malanjkhand Granite samples collected at varying distances from the CIS, to draw inferences about the above-mentioned time-relationship.

To fulfill the above objective, a total of 11 oriented granite samples were selected along a NW–SE-oriented corridor within the Malanjkhand Granite (Figure 1 *b*). This corridor is oriented perpendicular to the strike of the CIS, which is NE–SW, and the samples were located at varying distances from the CIS (Figure 2). Thin sections parallel to the magnetic foliation plane were prepared for each sample. The former was identified through anisotropy of magnetic susceptibility investigations of the samples. The intensity of SPO was quantified by calculating the

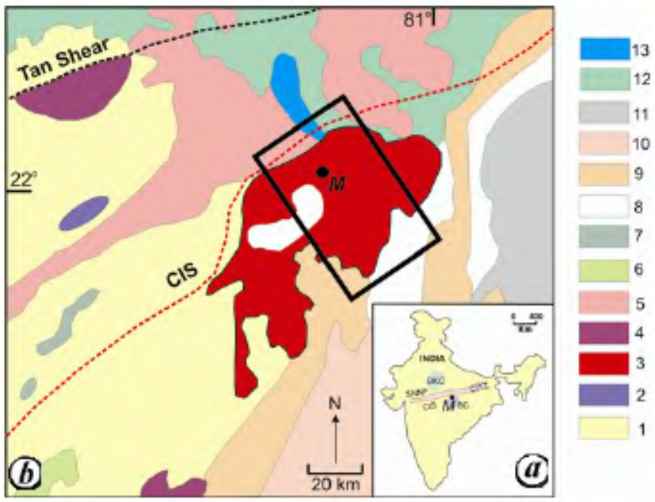

Figure 1. ***a***, Map of India highlighting the position of Malanjkhand Granite (M) that lies to the south of the Central Indian Tectonic Zone (CITZ). The northern and southern margins of the latter are demarcated by the Son–Narmada–North–Fault (SNNF) and the Central Indian Suture (CIS) respectively. BKC and BC represent Bundelkhand craton and Bastar craton respectively, that accreted during the Palaeoproterozoic and led to formation of the CITZ[10]. ***b***, General geological map of the area around Malanjkhand Granite (Jain *et al.*[23]). The rectangular box in the Malanjkhand Granite highlights the NW–SE-oriented corridor within which detailed sampling has been done for the present study. The sample locations along this corridor are shown in Figure 2. 1, Unclassified gneiss and granite; 2, Mahakoshal Group; 3, Malanjkhand Granite and equivalents; 4, Dongargarh granite and equivalents; 5, Sausar Group; 6, Sakoli Group; 7, Granulites of Sausar belt; 8, Chilpi Group; 9, Nandgaon Group; 10, Khairagarh Group; 11, Chhatishgarh Group; 12, Deccan Basalt flows and intrusives, and 13, Laterite and bauxite.

strength of mineral lineation defined by biotite grains in the granite thin sections. This was done by calculating the concentration parameter for biotite grains (κ_{bi}) using the Excel Worksheet of Piazolo and Passchier[19]. Statistical details about the concentration parameter (κ) have been provided in earlier studies[19,20]. The following procedure was followed. A frame in plane-polarized light from an oriented thin section was captured using a Leica DFC-320 digital camera attached to a Leica DMLP research microscope. Using Leica Qwin software, biotite grains in the frame were binarized, and the angle (α) between the longest axis of each biotite and E–W axis of the microscope stage was automatically determined (Figure 3). The aspect ratio (long to short axis ratio, R_{bi}) of each binarized biotite was also determined using the same software. To have a statistically significant number of biotite grains from every sample (thin section), it was necessary to capture several frames without changing the orientation of the slide with reference to the E–W axis of the microscope stage. Since the thin section was fitted within an *XY*-object guide on the microscope stage, an identical orientation was maintained while capturing various frames from the same thin section. The above procedure of binarizing biotite grains followed by measurement of α and R_{bi} was repeated for every frame. The results are given in Table 1.

According to Piazolo and Passchier[19], if $\kappa_{bi} \geq 0.20$, then the rock can be considered to have a statistically significant mineral lineation (SPO). As shown in Table 1 and Figure 4 *a*, all the 11 granite samples investigated in the present study have $\kappa_{bi} > 0.20$, and thus have a significant SPO. The exact perpendicular distance of each sample from the CIS (D_c) is listed in Table 1. To evaluate the variation in κ_{bi} with increasing distance from the CIS, the authors have prepared a D_c vs κ_{bi} plot (Figure 4 *b*). κ_{bi} was found to increase with a decrease in D_c. Thus, there is a negative correlation between κ_{bi} and D_c. To determine the significance of this correlation, the authors have calculated the Pearson's product moment correlation coefficient (r) for the D_c vs κ_{bi} plot. A value of 0.692 was obtained for the same. Since the number of samples (n) is 11, the degree of freedom is 9 ($n - 2$). With this value of degree of freedom, a minimum theoretical r value of 0.602 is necessary to consider the correlation as statistically significant at 95% confidence level (calculated using the url: http://secamlocal.ex.ac.uk/people/staff/dbs202/cat/stats/corr.html). Since the r value for the D_c vs κ_{bi} plot is 0.692 (i.e. > the theoretical r of 0.602 at 95% confidence level), it is concluded that the correlation is statistically significant and cannot be considered to be on account of chance. Since the northern part of the Malanjkhand Granite has proximity to the CIS, it is logical to infer that the former underwent greater strain. Therefore, the increase in SPO towards the CIS is inferred to be on account of increasing strain.

Data related to aspect ratio of biotite (R_{bi}) grains in the 11 samples analysed are listed in Table 1. The sample closest to the CIS has a median R_{bi} value of 2.1, while the sample farthest from the CIS has a median R_{bi} of 1.5. Figure 4 *c* is a κ_{bi} vs median R_{bi} plot. The correlation coefficient of the same is 0.76 and it indicates the tendency of biotite grains to become more elongated towards the CIS. This is also inferred to indicate greater strain in the samples proximal to the CIS. It is known that competent elliptical objects having aspect ratio (R) ≥ 3 get more strained than circular objects with the same viscosity[21]. As a consequence, under a given bulk strain, objects with $R \geq 3$ develop a stronger SPO than shorter grains. However, as noted from Table 1, in the present case of biotite grains from the Malanjkhand Granite, the mean as well as median R_{bi} for each sample are much lower than 3 and mostly <2. Therefore, the role of aspect ratio in causing difference in SPO in different parts of the granite is con-

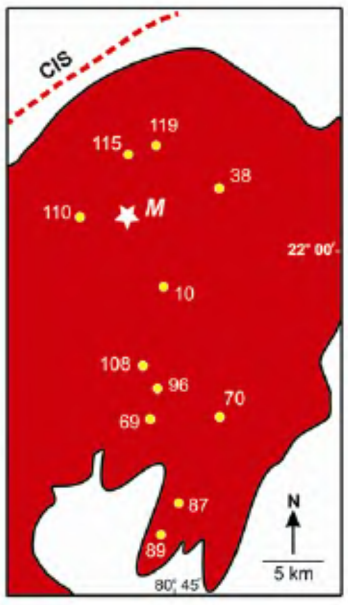

Figure 2. Map showing locations of samples in the Malanjkhand Granite in which shape preferred orientation analyses were done by measuring the strength of biotite mineral lineation.

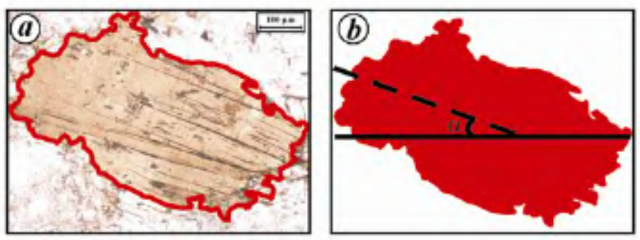

Figure 3. ***a***, Photomicrograph of a biotite grain in a thin section of Malanjkhand Granite. The outline of the grain has been highlighted. ***b***, Binarized biotite grain shown in (***a***). α is the angle between the E–W axis (solid line) of the microscope stage and longest axis of the biotite grain (dashed line). α was measured automatically for each binarized biotite grain using Leica Qwin software.

Table 1. Biotite shape preferred orientation data from the Malanjkhand Granite

Sample no.	n	D_c (km)	κ_{bi}	R_{bi}		
				Mean-R_{bi}	SD	Median-R_{bi}
115	40	08.10	1.121	2.20	0.61	2.1
119	62	09.00	0.605	1.87	0.57	1.8
110	85	09.50	0.799	2.03	0.61	1.9
38	27	14.90	0.623	1.74	0.38	1.6
10	50	18.00	0.311	1.77	0.49	1.7
108	35	22.05	0.429	1.71	0.63	1.5
96	34	24.30	0.480	1.76	0.40	1.8
69	47	25.20	0.478	1.50	0.32	1.4
70	29	28.80	0.579	1.60	0.37	1.5
87	44	31.81	0.370	1.70	0.42	1.5
89	46	33.18	0.411	1.70	0.46	1.5

n, Number of biotite grains studied in each sample. D_c, Distance of each sample from the CIS. κ_{bi}, Strength of mineral lineation defined by biotite. R_{bi}, Aspect ratio of biotite.
The statistical mean with standard deviation (SD) and median of R_{bi} are also tabulated.

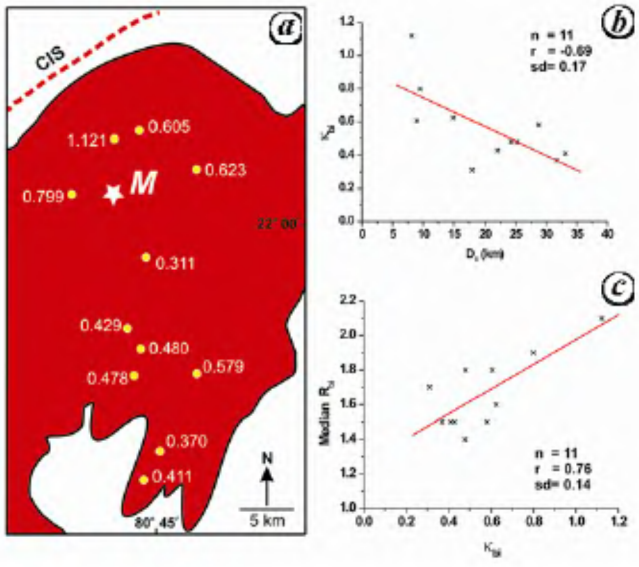

Figure 4. ***a***, Map showing values of strength of mineral lineation (κ_{bi}) for the 11 samples analysed in the present study. ***b***, D_c vs κ_{bi} plot for the samples analysed, where D_c is the distance of a sample from the CIS measured perpendicular to the strike of the CIS. ***c***, κ_{bi} vs median R_{bi} plot for the analysed samples. The linear regression line is shown in red. The Pearson's product moment correlation coefficient (r) and its standard deviation (sd) are also shown.

sidered negligible and strain associated with tectonic events in the vicinity of CIS is considered the dominant factor responsible for high SPO in the northern part of the Malanjkhand Granite. This also implies that the increase in κ_{bi} towards the CIS leads to identification of increasing strain towards the CIS. Thus, the tectonic events that led to the formation/rejuvenation of the CIS have influenced fabric development in the Malanjkhand Granite.

The present study also leads to a better understanding of regional Proterozoic tectonic events that occurred in Central India. As discussed earlier, the timing of CIS formation has been debated in the past. Palaeomagnetic measurements on 1800 and 2500 Ma volcanics that lie to the north and south of the CIS revealed a similar pole position for the rocks of 1800 Ma and different pole position for the rocks of 2500 Ma, thus leading to the conclusion[12,13] that the collision between the Bundelkhand and Bastar cratons took place between 2500 and 1800 Ma. In contrast, some studies have concluded that the formation of CIS took place during the ~1.5 Ga tectonothermal events that occurred along the CITZ[11]. Since the granite has magmatic fabrics (preferentially oriented feldspar laths) and high-T solid-state deformation fabrics (chessboard pattern in quartz), it can be concluded that the emplacement and initial fabric development in the granite was synchronous with regional tectonics. Since the age of the granite is ~2.48 Ga and the accretion of Bundelkhand and Bastar cratons also initiated during the Palaeoproterozoic, it is inferred that the initial high-T fabric development in the granite was synchronous with initiation of the above accretion. However, there is a superimposition of low-T over high-T fabric in the granite (particularly northern part that is close to CIS) and the intensity of SPO also increases towards the CIS. In light of the uncertain timing of CIS formation, two possible tectonic scenarios can be discussed.

First, the granite emplaced at ~2.48 Ga and developed high-T followed by low-T fabrics in a continuum. It is known that large, igneous intrusions cool on a timescale which is shorter than 10^5 years after emplacement[22]. Therefore, if low-T fabric developed in a continuum following high-T fabric development, then the process would have been completed within the Palaeoproterozoic itself. Because the SPO intensity as well as low-T fabric increase towards the CIS, this would imply that the formation of CIS would have occurred in the Palaeoproterozoic. This inference would support the findings based on palaeomagnetic studies[12,13] that the CIS formed between 2.5 and 1.8 Ga.

Second, the granite emplaced and solidified around ~2.48 Ga synchronously with the initial accretionary process associated with the evolution of the CITZ. At this stage high-T fabrics dominated throughout the Malanjkhand Granite. At a subsequent stage (and age), the granite was remobilized during which low-T fabrics superimposed on the high-T fabrics. From previous studies tectonothermal events at ~1.8, ~1.5 and ~1.1 Ga are known from the CITZ, and the CIS is known to have developed during the 1.5 Ga event[11]. Therefore, if the second possibility was correct, then the superimposition of low-T over high-T fabric and mylonitization in the northern part of the granite would have taken place in the Mesoproterozoic. Thus, the timing of CIS formation needs to be better constrained, for which further geochronological investigation of the rocks in the vicinity of CIS is necessary.

1. Archanjo, C. J., Bouchez, J. L., Corsini, M. and Vauchez, A., The Pombal granite pluton: magnetic fabric, emplacement and relationships with the Brasiliano strike-slip setting of NE Brazil (Paraiba State). *J. Struct. Geol.*, 1994, **16**, 323–336.
2. Bouchez, J.-L., Granite is never isotropic: an introduction to AMS studies of granitic rocks. In *Granite: From Segregation of Melt to Emplacement Fabrics* (eds Bouchez, J. L., Hutton, D. W. H. and Stephens, W. E.), Kluwer, Dordrecht, 1997, pp. 95–112.
3. Ferré, E., Gleizes, G. and Caby, R., Obliquely convergent tectonics and granite emplacement in the Trans-Saharan belt of Eastern Nigeria – a synthesis. *Precambrian Res.*, 2002, **114**, 199–219.
4. Benn, K., Paterson, S. R., Lund, S. P., Pignotta, G. S. and Kruse, S., Magmatic fabrics in batholiths as markers of regional strains and plate kinematics: example of the cretaceous Mt Stuart Batholith. *Phys. Chem. Earth, Part A*, 2001, **26**, 343–354.
5. Archanjo, C. J., Trindade, R. I. F., Bouchez, J. L. and Ernesto, M., Granite fabrics and regional-scale strain partitioning in the Seridó belt (Borborema Province, NE Brazil). *Tectonics*, 2002, **21**, DOI: 10.1029/2000TC001269.
6. Mamtani, M. A. and Greiling, R. O., Granite emplacement and its relation with regional deformation in the Aravalli Mountain Belt (India) – inferences from magnetic fabric. *J. Struct. Geol.*, 2005, **27**, 2008–2029.
7. Sen, K., Majumder, S. and Mamtani, M. A., Degree of magnetic anisotropy as a strain intensity gauge in ferromagnetic granites. *J. Geol. Soc. London*, 2005, **162**, 583–586.
8. Sen, K. and Mamtani, M. A., Magnetic fabric, shape preferred orientation and regional strain in granitic rocks. *J. Struct. Geol.*, 2006, **28**, 1870–1882.
9. Panigrahi, M. K., Bream, B. R., Misra, K. C. and Naik, R. K., Age of granitic activity associated with copper–molybdenum mineralization at Malanjkhand, Central India. *Miner. Deposita*, 2004, **39**, 670–677.
10. Yedekar, D. B., Jain, S. C., Nair, K. K. K. and Dutta, K. K., The central Indian collision suture. *Geol. Surv. India, Spec. Publ.*, 1990, **28**, 1–43.
11. Roy, A., Hanuma Prasad, M. and Bhowmik, S. K., Recognition of Pre-Grenvillian and Grenvillian Tectonothermal events in the Central Indian Tectonic zones: implications on Rodinian Crustal Assembly. *Gondwana Res.*, 2001, **4**, 755–757.
12. Rao, G. V. S. P. and Mishra, D. C., A Proterozoic APWP of cratons from either side of Narmada–Son lineament. In Proceedings of a Workshop on the Tectonics of the 'Narmada–Son Lineament'. Geol. Surv. India, Calcutta, Misc. Publ., 1997, vol. 63.
13. Mishra, D. C., Singh, B., Tiwari, V. M., Gupta, S. B. and Rao, M. B. S. V., Two cases of continental collisions and related tectonics during the Proterozoic period in India – insights from gravity modelling constrained by seismic and magnetotelluric studies. *Precambrian Res.*, 2000, **99**, 149–169.
14. Vigneresse, J. L., Barbey, P. and Cuney, M., Rheological transitions during partial melting and crystallisation with application to feldsic magma segregation. *J. Petrol.*, 1996, **37**, 1579–1600.
15. Vigneresse, J. L., Rheology of a two-phase material with applications to partially molten rocks, plastic deformation and saturated soils. In *Flow Processes in Faults and Shear Zones* (eds Alsop, G. I., Holdsworth, R. E. and McCaffrey, K. J. W.), Geol. Soc., London, Spec. Publ, 2004, **224**, 79–94.
16. Kruhl, J. H. and Nega, M., The fractal shape of sutured quartz grain boundaries: application as a geothermometer. *Geol. Rundsch.*, 1996, **85**, 38–43.
17. Blenkinsop, T. J., *Deformation Microstructures and Mechanisms in Minerals and Rocks*, Kluwer, Drodrecht, 2000.
18. Stipp, M., Stünitz, H., Heilbronner, R. and Schmid, S. M., The eastern Tonale fault zone: a natural laboratory for crystal plastic deformation of quartz over a temperature range from 250 to 700°C. *J. Struct. Geol.*, 2002, **24**, 1861–1884.
19. Piazolo, S. and Passchier, C. W., Controls on lineation development in low to medium grade shear zones: a study from the Cap de Creus peninsula, NE Spain. *J. Struct. Geol.*, 2002, **24**, 25–44.
20. Masuda, T., Kugimiya, Y., Aoshima, I., Hara, Y. and Ikei, H., A statistical approach to determination of mineral lineation. *J. Struct. Geol.*, 1999, **21**, 467–472.
21. Treagus, S. H. and Treagus, J. E., Effects of object ellipticity on strain, and implications for clast–matrix rocks. *J. Struct. Geol.*, 2001, **23**, 601–608.
22. McKenzie, D., The extraction of magma from the crust and mantle. *Earth Planet Sci. Lett.*, 1985, **74**, 81–91.
23. Jain, S. C., Yedekar, D. B. and Nair, K. K. K., A review of the stratigraphic status of Bharweli–Ukwa manganese belt, Balaghat, Madhya Pradesh. *Geol. Surv. India Misc. Publ.*, 1990, **28**, 332–353.

ACKNOWLEDGEMENTS. S.M. acknowledges financial support from the Indian Institute of Technology, Kharagpur in the form of an Institute Research Scholarship to pursue his doctoral research on the Malanjkhand Granite. Discussions with M. K. Panigrahi and Saibal Gupta, and comments by the anonymous referee were useful.

Received 26 April 2008; revised accepted 6 November 2008